A R C H I V E S O F M E T A L L U R G Y A N D M A T E R I A L S
Volume 60 2015 Issue 3
DOI: 10.1515/amm-2015-0330

B. MRZYGŁÓD*,#, A. KOWALSKI**, I. OLEJARCZYK-WOŻENSKA*, H. ADRIAN*, M.GŁOWACKI*, A. OPALIŃSKI*

EFFECT OF HEAT TREATMENT PARAMETERS ON THE FORMATION OF ADI MICROSTRUCTURE WITH ADDITIONS OF Ni, Cu, Mo

WPŁYW PARAMETRÓW OBRÓBKI CIEPLNEJ NA KSZTAŁTOWANIE MIKROSTRUKTURY ŻELIWA ADI Z DODATKAMI Ni, Cu, Mo

Metallographic examinations and mechanical tests were carried out on the ductile iron with additions of Ni, Cu and Mo in as-cast state and after austempering. TTT and CCT diagrams were plotted. The heat treatment was performed in six different variants. Studies included qualitative assessment of the microstructure and testing of mechanical properties such as $R_{0,2}$, R_m, A, Z, HRC, KC. An analysis of the obtained results was also presented.
Keywords: ductile iron, heat treatment, the microstructure of ADI, ADI mechanical properties

Przeprowadzono badania metaloznawcze żeliwa sferoidalnego z dodatkami Ni, Cu i Mo w stanie lanym i po hartowaniu izotermicznym. Opracowano wykresy CTPi i CTPc. Obróbkę cieplną wykonano w sześciu różnych wariantach. Badania metaloznawcze obejmowały ocenę jakościową mikrostruktury i pomiary właściwości mechanicznych: $R_{0,2}$, R_m, A, Z, HRC, KC. Dokonano analizy uzyskanych wyników

1. Introduction

ADI (Austempered Ductile Iron) offers a very favourable combination of high strength, high ductility and fracture toughness. It is obtained as a result of the properly performed heat treatment (austempering) of ductile iron. A diagram of the process conducted to obtain ADI is presented in Fig. 1.

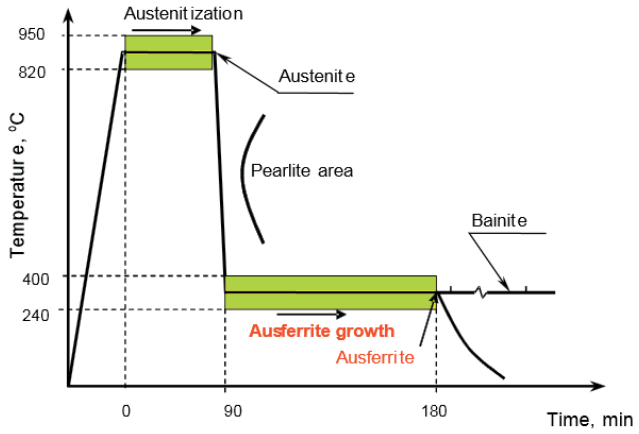

Fig. 1. Heat treatment steps to obtain ADI

The essence and purpose of the heat treatment of ductile iron is to rebuild its base structure, in most cases with pearlitic matrix, and obtain the cast iron with an ausferritic matrix (a mixture of stable austenite and plate-shaped ferrite in the form of "needles"). The type of the obtained structure mainly depends on the chemical composition of ductile iron and heat treatment parameters. ADI structure determines the obtained mechanical properties, hardness, strength, ductility, etc. An important tool to help optimise the structure and properties of iron alloys are the methods of computer modelling of phase transformations occurring during heating and cooling [1-4]. Computer modelling also plays an important role in predicting the structure and properties of the alloy after casting process [5].

2. ADI chemical composition in the light of literature

The development of ADI forced some changes in the chemical composition of the base cast iron, mainly as regards the type of the alloying elements added. Alloying elements are introduced into the ausferritic ductile iron to increase its hardenability, since unalloyed cast iron can be hardened only through a thickness of approx. 20 mm. The ADI hardenability is the ability of the alloy to cool

* AGH UNIVERSITY OF SCIENCE AND TECHNOLOGY, AL. A.MICKIEWICZA 30 30-059 KRAKOW, POLAND
** FOUNDRY RESEARCH INSTITUTE, 73 ZAKOPIAŃSKA STR., 30-418 KRAKOW, POLANAA
# Corresponding author: mrzyglod@agh.edu.pl

sufficiently quickly to avoid the formation of pearlite and the ability to form a uniform ductile microstructure composed of plate-like ferrite and stable austenite, while held at the bainitic transformation temperature. The hardenability of this cast iron largely depends on the temperature of bainitic (ausferritic) transformation. This was confirmed by R. Darwish and R. Elliot [6].

Nomograms showing the impact of various alloying elements on the critical diameter D_c were also developed [7]. By critical diameter is meant the largest diameter of the sample after austempering at a temperature T_{PI}, free from pearlite precipitates in the middle of the section. This diameter can be calculated from Equation (1) [8]:

$$Dc = 124\ C\gamma + 27(\%Si) + 22(\%Mn) + 16(\%Ni) + 25(\%Mo) - 1.68\ x\ 10^{-4} T^2_{PI} + 12(\%Cu)(\%Ni) + 62(\%Cu)(\%Mn) + 88(\%Ni)(\%Mo) + 11(\%Mn)(\%Cu) + 127(\%Mn)(\%Mo) - 20(\%Mn)(\%Ni) - 137 \quad (1)$$

where C_γ - is carbon content in austenite, and the symbols of elements represent their respective content in % by weight. The carbon content in austenite C_γ is calculated from Equation (2):

$$C\gamma = T\gamma\ /420 - 0.17(\%Si) - 0.95 \quad (2)$$

where: T_γ is the temperature of austenitising in °C.

The most effective additives increasing the hardenability of ductile iron include molybdenum, nickel, copper, and manganese. It has long been known that the effect of one alloying element on the hardenability is significantly weaker than the simultaneous effect of two or three elements [9]. Therefore, research was conducted on the cast iron with different combinations of alloying elements such as Ni-Mo, Ni-Cu-Mo, Cu-Mo, Ni-Cu, Mn-Cu [10-12]. ADI containing 1.5% Ni and 0.3% Mo soon gained worldwide popularity and widespread use in industry; various studies were also conducted on this material. J.F. Janowak and P.A. Morton in their work [13] have examined in detail the effect of austempering conditions on the mechanical properties of this cast iron.

M. Grech and J.M. Young [10] have investigated the ADI containing 1.6% Ni and 1.6% Cu. The best combination of the tensile strength (R_m = 1035 MPa) and ductility (A = 11%) was obtained upon austempering in the temperature range of 350 - 375°C.

The nickel-copper-molybdenum cast iron was used for crankshafts operating in four-cylinder petrol engines with a power of 100 HP and in one-cylinder diesel engines with a power of 70 HP [14]. The cast iron had the following composition: 3.45-3.55% C, 2.5-2.7% Si, 0.25-0.30% Mo, 0.95-1.0% Ni, 0.5-0.6% Cu. This composition was intended to provide a good enough cast iron hardenability during heat treatment with isothermal transformation. The results of tests conducted on the nickel - copper cast iron containing 3.52% C, 2.87% Si, 0.22% Mn, 0.051% Mg, 1.55% Ni, 0.73% Cu as described in [15] are given in Table 1.

TABLE 1

Mechanical properties of nickel - copper ADI austempered at different temperatures and austenitised at 900°C for 2h

Property	Temperature of austempering treatment, °C (time 2h)					
	280	300	320	340	360	380
Rm, MPa	1476	1353	1298	1239	1061	1056
A, %	5.5	6.5	8.3	7.2	13.3	13.5
HB	419	389	382	365	317	314

The copper – molybdenum cast iron has also found some applications in the industry [16,17]. For example, [17] describes the use of cast iron of the following composition: 3.50% C, 2.90% Si, 0.265% Mn, 0.08% P, 0.039% Mg, 0.028% Ce, 0.62% Cu, 0.19% Mo. It was used for the automotive ring and hypoid gears of the rear axle. The cast iron showed a good fatigue resistance in the range of 310 - 350 MPa; other mechanical properties obtained were as follows: R_m = 1300 - 1500 MPa, *KCU* = 66 - 100 J, *HRC* = 46 - 49. Several works were devoted to the cast iron with increased content of Mn (0.7 - 1.0%) [18-21]. Attempts were also made to study ductile iron with the addition of vanadium [22] and boron [23], but comprehensive data on properties of these cast irons are not available.

There are also works that are intended to produce a new grade of carbide-enriched ductile iron with different metal matrix microstructure. This cast iron is obtained by the Inmold process, where the desired microstructure of the metal matrix is formed without the use of heat treatment (in as-cast condition) only by suitable quantitative combination of alloying elements. [24, 25].

A review of the literature shows that the Ni-Cu-Mo cast iron has been tested to a relatively small extent, and therefore this work is a partial complement to this issue. The aim of the present study was to analyse the effect of heat treatment that transforms ordinary ductile iron into ADI on the microstructure and mechanical properties of the Ni-Cu-Mo cast iron. Respective CCT and TTT diagrams were also developed for this cast iron.

3. Test materials and methods

3.1 Test materials

Studies were conducted on low-alloy ductile iron with the chemical composition given in Table 2. The cast iron contained 1.2% Ni, 0.7% Cu and 0.2% Mo.

TABLE 2

Chemical composition of the tested cast iron, in mass %

C	Si	Mn	P	S	Mg	Ni	Cu	Mo
3.57	2.13	0.26	0.06	0.015	0.038	1.2	0.7	0.2

Melting was conducted in a RADYNE medium-frequency induction furnace with 100 kg capacity crucible and an inert

lining. The cast iron spheroidising treatment was performed by Sandwich process in a slender ladle at a temperature of 1400°C. From the ductile iron, sample ingots were cast according to EN 1564 – Fig. 2.

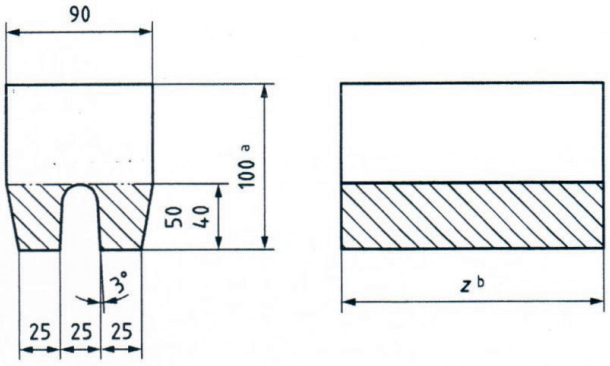

Fig. 2. Separately cast test sample type IIb (EN 1564)

Test specimens were cut out from the lower part of ingots. They were austempered following the previously established variants of heat treatment.

The tested cast iron had a eutectic composition. This composition is optimal for ductile iron, since at the lowest shrinkage it provides sound castings free of hard spots, internal defects, or graphite flotations.

3.2 Heat treatment

The heat treatment process included: austenitising of ductile iron at 850, 900, 950°C for 2 hours followed by austempering in the temperature range of 280 - 380°C for a variable time of 1.5 to 3h. Detailed comparison of heat treatment variants is presented in Table 3.

TABLE 3

Variants of the performed heat treatment

Heat treatment variant	Austenitising		Austempering	
	T_A, °C	t_A, h	T_{PI}, °C	t_{PI}, h
ADI-850/2/280/3	850	2	280	3
ADI-850/2/300/3	850	2	300	3
ADI-900/2/320/2	900	2	320	2
ADI-900/2/340/2	900	2	340	2
ADI-950/2/360/1,5	950	2	360	1.5
ADI-950/2/380/1,5	950	2	380	1.5

Samples were austenitised in a Multitherm N41/M Nabertherm furnace with the sealed retort and a protective atmosphere of inert gas (argon), preventing the sample surface decarburisation. Austempering was carried out in a PEW-2 bath-type electric furnace in a salt bath composed of a mixture of potassium nitrate and sodium nitrite.

3.3 Analysis of microstructure

To reveal the microstructure of the tested material, metallographic sections were prepared for both as-cast ductile iron and ADI samples after different variants of heat treatment.

Metallographic sections in as-cast state were etched in the Mi1Fe reagent (4% nital) according to PN-61 / H-04503.

Metallographic sections of ADI (after heat treatment) were etched in the B-M reagent of the following chemical composition: 100 ml of base solution (5 parts by volume H_2O, 1 part by volume HCl conc.), 2 g of $NH_4F \cdot HF$, 1 g $K_2S_2O_5$. This reagent does not colour austenite and carbides, but it colours bainite and tempered martensite in brown and martensite in blue. Sometimes fine needles of martensite are not coloured in blue but in light brown, and then in the assessment of the microstructure, their morphology should be taken into account. Both as-cast and heat-treated microstructures were examined under an AXIO OBSERVER Z1M metallographic microscope. The study of the microstructure of graphite was carried out by comparing the microstructure of non-etched samples with patterns contained in the PN-EN ISO 945-1: 2009. Examination of the microstructure of metal matrix was carried out by comparing the microstructure of etched samples with patterns of microstructure contained in the PN - 75 / H-04661.

3.4 Testing of mechanical properties

Testing of mechanical properties included:

- *static tensile test at ambient temperature* – the tensile test was performed in accordance with PN-EN 10002-1: 2004 using an EU-20 testing machine made by FEB Werkstoffprufmaschinen Leipzig. The stress increment rate during test was 1.59 MPa/s, the loading force was 1471 N, and the nominal load duration was 4 s. The following parameters were determined in the test: the tensile strength - R_m, the elongation - A and the reduction of area-Z,
- *measurement of Charpy impact resistance* at ambient temperature in accordance with PN-EN 10045-1: 2007. The Charpy pendulum impact tester with an initial energy K_{max}=150 J or 300 J was available. The 150 J pendulum was used in the tests,
- *hardness measurement* - hardness was measured in Rockwell C, type Zwick/Roell ZHU 250, scale in accordance with PN-EN ISO 6508-1: 2007.

Testing of mechanical properties and impact resistance was carried out on three samples for each variant of the heat treatment and on three samples of ductile iron in as-cast state. Hardness was measured on specimens that failed in the static tensile test. The results presented in the following part of the study represent average values calculated from the three measurements taken for each cast iron variant.

3.5 Dilatometric studies

Dilatometric tests were performed using a High Speed Quenching Dilatometer, model RITA L78 made by LINSEIS. The analysis of experimental data and plotting of TTT and CCT diagrams were based on metallographic examinations and measurements of hardness HV30, performed on selected samples. Ductile iron samples with dimensions of φ3×10 mm austenitised at 900°C for a period of 30 minutes were used in the studies.

4. Test results

4.1 As-cast microstructure of ductile iron

Images of as-cast ductile iron microstructure are shown in Fig. 3. The microstructure is composed of metal matrix with particles of spheroidal graphite distributed in this matrix. Most of the graphite particles are surrounded by polygonal ferrite grains. The metal matrix is formed of pearlite, inside which occasionally occur ferrite grains and particles of non-metallic inclusions.

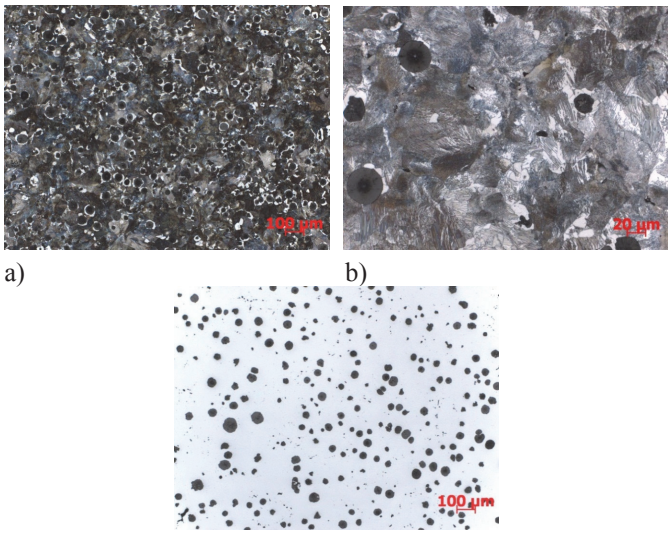

a) b)

c)

Fig. 3. As-cast microstructure of ductile iron, a) metallographic section etched with Mi1Fe, 100x; b) metallographic section etched with Mi1Fe, 500x, c) unetched metallographic section, 100x

4.2 Microstructure of ADI after different variants of austempering

Examples of heat-treated microstructure are shown in Fig. 4-9. The microstructure of cast iron consists of a matrix, which is a mixture of acicular ferrite and austenite with spheroidal graphite particles randomly distributed therein.

Careful analysis of the results shows that with the increasing temperature of isothermal transformation, the "needles" of lamellar ferrite becomes coarser. Ferrite nucleates on the austenite grain boundaries, which act as privileged sites for heterogeneous nucleation. At lower temperatures of the isothermal transformation, carbon diffusion is slower, and ferrite growth is retarded, resulting in the formation of more fine-grained ferrite. At higher temperatures, the growth of ferrite is more intense and, consequently, the individual plates of ferrite are larger but their overall volume decreases. In the case of austenite, its volume is smaller at lower temperatures, while at higher temperatures, the amount of unreacted austenite increases. Table 4 presents the results of quantitative analysis of the cast iron microstructure after heat treatment.

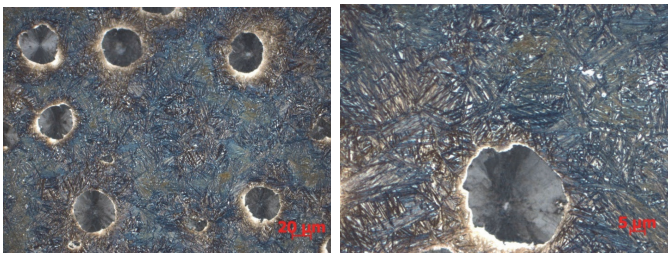

a) b)

Fig. 4. Microstructure of ductile iron after austempering, variant ADI-850/2/280/3, a) 500x, b) 1600x

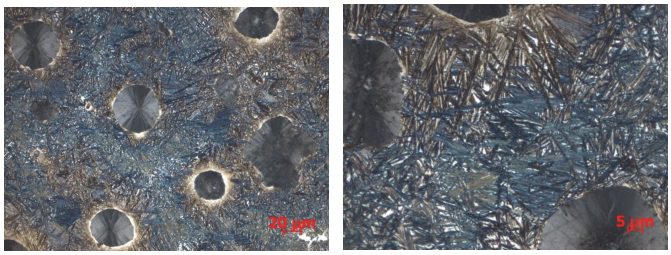

a) b)

Fig. 5. Microstructure of ductile iron after austempering, variant ADI-850/2/300/3, a) 500x, b) 1600x

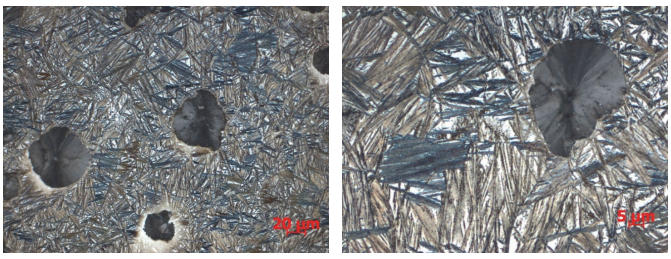

a) b)

Fig. 6. Microstructure of ductile iron after austempering, variant ADI-900/2/320/2, a) 500x, b) 1600x

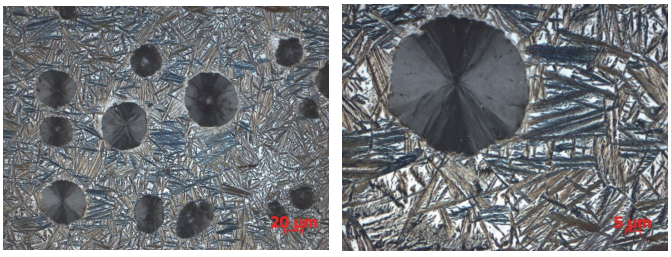

a) b)

Fig. 7. Microstructure of ductile iron after austempering, variant ADI-900/2/340/2, a) 500x, b) 1600x

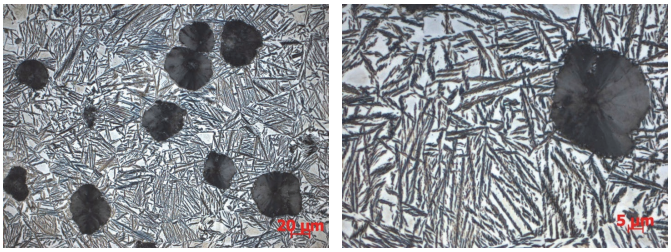

a) b)

Fig. 8. Microstructure of ductile iron after austempering, variant ADI-950/2/360/1,5, a) 500x, b) 1600x

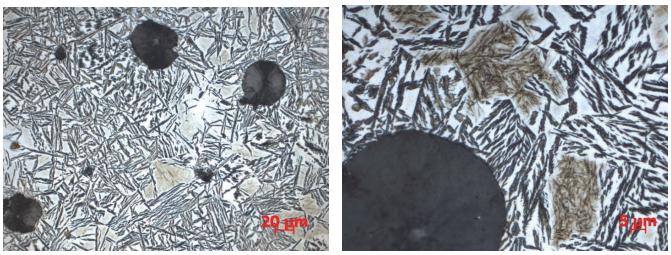

a) b)

Fig. 9. Microstructure of ductile iron after austempering, variant ADI-950/2/380/1,5, a) 500x, b) 1600x

TABLE 4

Structural constituents of ADI subjected to different variants of heat treatment

Heat treatment variant	Graphite	Metal matrix
ADI-850/2/280/3	80%VI6 + 20%V6	F + approx. 3%A
ADI-850/2/300/3	75%VI6 + 25%V6	F + approx. 7%A
ADI-900/2/320/2	80%VI6 + 20%V6	F + approx.10%A
ADI-900/2/340/2	80%VI6 + 20%V6	F + approx.10%A
ADI-950/2/360/1,5	80%VI6 + 20%V6	F+ approx. 15%A
ADI-950/2/380/1,5	70%VI6 + 30%V6	F + approx. 20%A
F –lamellar ferrite in the form of "needles", A – austenite		

b)

4.3 Testing of mechanical properties

4.3.1 As-cast mechanical properties of ductile iron

Ductile iron in as-cast state was characterised by the following mechanical properties: R_e=557 MPa, R_m=842 MPa, A=6,9 %, K_C=29.7 J. The examined cast iron had very high as-cast strength (over 800 MPa) and elongation (up to 10%). The $R_{p0.2}$ / R_m ratio was in the range of 0.63 - 0.69 and was typical for the ductile iron. The resulting mechanical properties are compared in Table 5.

TABLE 5

As-cast mechanical properties of ductile iron

No.	$R_{p0,2}$, MPa	R_m, MPa	$R_{0,2}/R_m$,	A, %	KCU, J
1	574	837	0.69	4.8	29
2	531	842	0.63	10	31
3	566	847	0.67	5.8	29
AVERAGE	**557**	**842**	**0.66**	**6.9**	**29.7**

4.3.2 Mechanical properties after heat treatment

Table 6 presents the results of mechanical tests carried out for the predetermined variants of heat treatment. The highest strength (1483 MPa) and hardness (43.4 HRC) were obtained for austempering at T_{PI} = 280°C. This cast iron can be used for castings operating under the conditions of dynamic abrasion. The best combination of strength and plastic properties was obtained for austempering at T_{PI} = 340°C (R_m = 1202 MPa and A = 6.5%). At T_{PI} = 380°C, the strength decreased to 862 MPa, which means that this temperature should not be used for the manufacture of cast iron with this composition. After treatment at 360°C, the cast iron had a high tensile strength (1032 MPa) combined with relatively low hardness (24.9 HRC) ensuring very good machinability. This is a great advantage, as it considerably facilitates the

TABLE 6

Mechanical properties obtained after different variants of heat treatment

Heat treatment variant	$R_{p0,2}$ MPa	R_m MPa	$R_{p0,2}/R_m$	A %	Z %	HRC	KCU J
ADI-850/2/280/3	1418	1486	0.95	1.0	0.5	43.4	40.1
ADI-850/2/300/3	1283	1430	0.90	1.7	1.7	39.3	56.2
ADI-900/2/320/2	1178	1205	0.98	2.4	2.0	36.6	62.2
ADI-900/2/340/2	1025	1202	0.85	6.5	5.4	32.7	79.4
ADI-950/2/360/1,5	780	1032	0.76	5.7	5.4	24.9	86.2
ADI-950/2/380/1,5	635	862	0.74	2.8	2.5	21.5	43.5

Vi,V - shape factors, 6 - size factor of grafite grains (PN-EN ISO 945 - 1:2009)

manufacture of castings, especially those with non-standard shapes. Particular attention deserves the extremely high ratio of yield strength to tensile strength amounting to 0.95; 0.90 and 0.98, especially after the treatment at temperatures of 280, 300 and 320°C, respectively. Such values are never obtained in the ordinary ductile iron, neither are they found in the recommendations for ADI covered by the PN EN 1564 standard.

The mechanical properties of cast iron as a function of austempering temperature are shown in graphic form in Fig. 10.

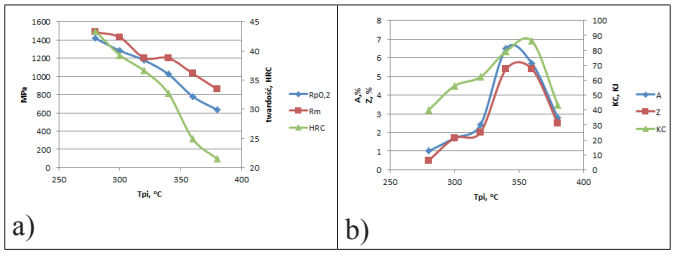

Fig. 10. Mechanical properties of ADI after various cycles of austempering, a) strength properties, b) plastic properties

4.4 The results of dilatometric studies

Fig. 11 shows a TTT diagram which illustrates the extent of phase stability as a function of the time of holding at a given temperature. It has been based on the curves of the transformation kinetics for different temperatures of ausferritising, indicating the start and end time of the transformation.

From Fig.11 it follows that the temperature of bainitic transformation is comprised in a range of 500 - 280°C. The TTT diagram shows two ranges of the bainite formation, i.e. 500 - 360ºC and 360 - 280°C. The former corresponds to the formation of upper bainite, and the latter to the formation of lower bainite. Detailed examination of this diagram leads to the conclusion that with the increasing austempering temperature, the rate of bainitic transformation and the content of austenite are also increasing. The data comprised in Table 5 show that with the temperature T_{PI} increasing in the bainitic range, the content of unreacted austenite is growing from 5% at a temperature of 280°C to 25% at a temperature of 400°C. At a temperature of 450°C, the content of austenite is lower and amounts to 20%.

From the TTT diagram it also follows that the temperature of the maximum rate of transformation of austenite to pearlite is approx. 615°C. The incubation period for pearlite transformation is approx. 120 seconds, and the incubation period for the transformation of austenite into upper bainite at 500°C is approx. 100 seconds. In contrast, the incubation period for the transformation of austenite into lower bainite at approx. 280°C is approx. 450 seconds. The completion of pearlitic transformation at 560°C takes place after the lapse of 600 seconds, of bainitic transformation at 350°C after 75 minutes, and of bainitic transformation at 280°C after approximately 2 hours. Martensitic transformation starts at a temperature of 210°C.

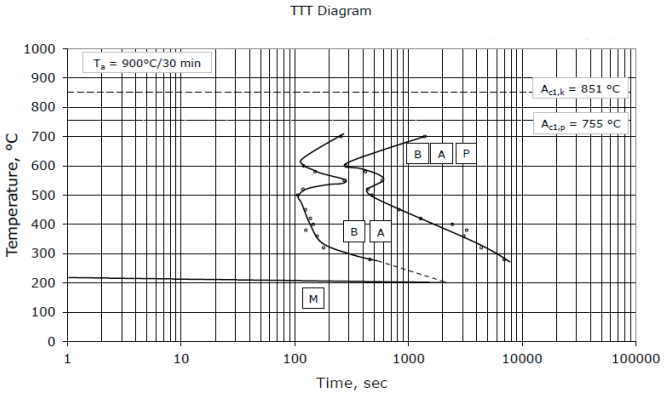

Fig. 11. TTT diagram, cast iron Ni-Cu-Mo

The content of individual phases in the metal matrix at each austempering temperature is shown in table 7.

TABLE 7

The contents of metal matrix phases

Austempering temperature T_{PI}, °C	**Microstructure of metal matrix**
280	B_l + 5% A
320	B_l + 10% A
360	B_l + 10%B_u +15% A
400	B_u+ 20% B_l + 25% A
450	B_u+ 10% B_l + 20% A
500	B_u + 2% A + (A + M) – at eutectic cell boundaries
550	B_u + 5%A + M (at eutectic cell boundaries)
600	B_u + 30% P + 2% A + M - at eutectic cell boundaries
B_l– lower bainite, B_u – upper bainite, M – martensite, A – austenite, P - pearlite	

Fig. 12 shows a CCT diagram with phase stability ranges during continuous cooling at a predetermined rate. The solid lines mark the beginning and end of transformation during continuous cooling of cast iron samples.

The CCT diagram shown in Figure 12 gives us the following information:

- in the temperature range of 800-400°C, two diffusion-based austenite transformations take place, i.e. austenite - ferrite and austenite - pearlite;
- the minimum incubation period necessary for austenite - ferrite transformation occurs at a temperature of 620°C and amounts to approx. 26 seconds;
- the minimum incubation period for austenite - pearlite transformation occurs at a temperature of 600°C and amounts to approx. 230 seconds;
- the temperature of the occurrence of pearlitic area is in the range of 730 - 580°C;
- the temperature of the occurrence of bainitic area is in the range of 400 - 180°C;
- the martensitic transformation starts at a temperature of 220°C and decreases with the increasing time of cooling.

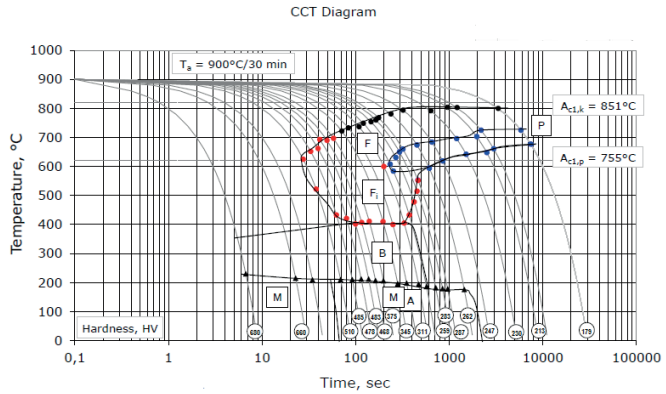

Fig. 12. CCT diagram, cast iron Ni-Cu-Mo

The contents of individual phases in the metal matrix for each cooling rate is presented in Table 8. The data comprised in this table clearly show how the structure of cast iron changes from ferrite into pearlite and martensite with the changing rate of cooling.

TABLE 8

Cast iron structure obtained as a result of different cooling rates

Sample cooling rate v, K/min	**Microstructure of metal matrix**
2	80%P + 20%F
45	70% P + 15% F + 20% (F_i +M + A)
75	30% P + 10% F + 40% (F_i + A + M) +20% B_l
255	60% M + 15% F_i + A) +25% B_l
300	70% M + 10% (F_i + A) +20% B_l
450	80% M + 10% (F_i + A) +10% B_l
600	90% M +10% B_l + (F_i + A) - traces
1800	M + F (traces)
B_l– lower bainite, M – martensite, P – pearlite, F – polygonal ferrite, F_i – acicular ferrite, A – austenite	

4.5 The hardenability

As mentioned in the introduction, ADI should offer good hardenability. For the present composition, the hardenability expressed as a value of the critical diameter D_c was calculated from Equation (1). The results of calculations are presented in Table 9.

TABLE 9

The critical diameter Dc for selected variants of heat treatment

Heat treatment variant	T_γ, °C	T_{pi}, °C	Cγ, %	D_c, mm
ADI-850/2/280/3	850	280	0.71	76
ADI-900/2/320/2	900	320	0.83	87
ADI-950/2/360/1,5	950	360	0.95	119

Analysing the data given in Table 7 it can be concluded that:

- the degree of austenite saturation with carbon increases with increasing temperature of the austenitising treatment: from 0.71% at T_γ = 850°C up to 0.95% at T_γ = 950°C;
- the critical diameter D_c as a measure of hardenability increases with the increasing temperature of austenitising and austempering, reaching its maximum for the austenitising temperature of 950°C and austempering temperature of 360°C.

5. Summary of test results

The examined ductile iron containing alloying additions in the amount of 1.2% Ni, 0.7% Cu and 0.2% Mo showed satisfactory mechanical properties in the as-cast state. Those properties were owed to the use of alloying additions and fully pearlitic microstructure of the matrix. Austempering from the austenitising temperature strongly influenced the change in mechanical properties. The yield strength $R_{p0.2}$ and the ultimate tensile strength R_m of the cast iron after austempering were in the ranges of 635-1418 and 862-1486 MPa, respectively, while the same as-cast properties were 557 and 842 MPa, respectively. High strength properties were accompanied by an increase in fracture toughness. The energy needed to fracture the as-cast iron specimens tested for the impact resistance was equal to 29 J, while for the same cast iron subjected to heat treatment it increased to the range of 40.1-86.2 J. For most of the heat treatment variants, the cast iron showed a lower value for elongation A as compared to the as-cast state. With the increase of austempering temperature T_{PI}, the values of the mechanical properties were decreasing. The ductility and impact resistance were increasing with the T_{PI} temperature increasing up to 360°C, but they decreased when this temperature was exceeded. Changes in the mechanical properties during austempering were associated with changes in the microstructure. The microstructure of austempered ductile iron was composed of a mixture of acicular (bainitic) ferrite and unreacted austenite. The fall of plastic properties and impact resistance at a temperature of 380°C can be explained by the fact that at this temperature, the transformation of austenite into upper bainite occurs, and below this temperature into lower bainite. To confirm this assumption, the use of electron microscopy is required to study the microstructure. Among the applied variants of the austempering treatment, the optimal one that provided high strength, high plastic properties and crack resistance has proved to be the variant of ADI-900/2/340/2, where the austenitising temperature Tγ, was 900°C and the austempering temperature was equal to 340°C. Maximum strength properties were obtained in the variant of ADI-850/2/280/3, but at the expense of impact resistance which, compared with the former variant, suffered a double drop.

The developed CCT and TTT diagrams of the tested cast iron are the source of valuable data that can be used in optimisation of the heat treatment parameters and as a supporting tool for computer modelling of these processes.

They also enrich our knowledge of phase transformations occurring during the heat treatment of low-alloy ductile iron.

Acknowledgments

The authors with to thank the Team of Ferrous Alloys Department in the Foundry Research Institute in Cracow for preparation of the test material and the Laboratory Staff of this Institute for the implementation of metallographic studies.

Financial assistance of the NCN, project No. 2013/11/N/ST8/00326

REFERENCES

[1] H. Adrian, Numerical modeling of heat treatment processes, Publishing AGH, Krakow (2011).

[2] I. Olejarczyk-Wożeńska, H. Adrian, B. Mrzygłód, Mathematical model of the process of pearlite austenitization, Archives of Metallurgy and Materials **59** (3), 981-986 (2014).

[3] I. Olejarczyk-Wożeńska, H. Adrian, A. Adrian, B. Mrzygłód, Parametric representation of TTT diagrams of ADI cast iron, Archives of Metallurgy and Materials **57**(2), 613-617 (2012).

[4] I. Olejarczyk-Wożeńska, A. Adrian, H. Adrian, B. Mrzygłód, Algorithm for controling of quench hardening process of constructional steels, Archives of Metallurgy and Materials **55** (1), 171-179 (2010).

[5] S. Kluska-Nawarecka, E. Nawarecki, B. Sniezynski, D. Wilk-Kolodziejczyk, The recommendation system knowledge representation and reasoning procedures under uncertainty for metal casting. Metalurgija **5** (1), 263-266 (2015).

[6] N. Darwish, R. Elliott, Austempering of low manganese ductile irons. Part 1. Processing window. Mat.. Science Technol. **9**, 572 (1993).

[7] E. Dorazil, High strength austempered ductile cast iron, Academia Prague (1991).

[8] L. Jincheng, R. Elliot, The influence of cast structure on the austempering o ductile iron. Part 3. The role of nodule count on the kinetics, microstructure and mechanical properties of austempered Mn alloyed ductile iron. International Journal of Cast Metals Research **12**, 189-195 (1999).

[9] R. Elliottt, Current status of austempered cast irons. Physical Metallurgy of Cast Iron V, France, s. 1, (1994).

[10] M. Grech, J.M. Young, Influence of austempering temperature on the characteristics of austempered ductile iron alloyed with Cu and Ni. AFS Transactions **98**, 345 (1990).

[11] Hua-Qin Su, Xing-Li Guo, J.M. Schissler, Influence of nickel on kinetics of bainitic transformation of the first stage of austempered ductile iron (ADI). 5th International Symposium on the Physical Metallurgy of Cast Iron, October 1994, Nancy, France, (1994).

[12] T.S. Shih, Z.Z. Hwang, C.Z. Wu, Optimisation of composition and dimensions in producing austempered ductile irons. Transactions AFS, 649 (1996).

[13] J.F. Janowak, P.A.Morton, A guide to mechanical properties possible by austempered 1,5% Ni-0,3% Mo ductile iron. Transactions AFS 1984, 489 (1984).

[14] M. Bahmani, R. Elliott, N. Varahram, Austempered ductile iron: a competitive alternative for forged induction hardened steel crankshafts. International Journal of Cast Metals Research **9**, 249 (1997).

[15] J. Tybulczuk, A. Kowalski, Characteristic of ADI with additions of 1,5% Ni and 0,8% Cu, Transactions of the Foundry Research Institute **4**, 403 (1997).

[16] Y.J. Park, P.A. Morton, M. Gagne, R. Goller, Continuous cooling transformation and austempering behavior of Cu-Mo ductile irons, Transactions AFS, 395 (1984).

[17] Ritzel und Tellerrader aus zwischenstufenvergüteten Gusseisen mit Kugelgraphit mit gegossenen zahnen. Giesserei **67**(8) 206 (1980).

[18] H., Bayati, R. Elliott, Influence of austenitising temperature on mechanical properties of high manganese alloyed ductile iron, Material Science and Technology **11**, 908 (1995).

[19] H. Bayati, R. Elliott, W. R.Lorimer, Stepped heat treatment for austempering of high manganese alloyed ductile iron. Material Science and Technology **11**, 1007 (1995).

[20] A., Kowalski, M. Biel-Gołaska, Shaping the structure and properties of ADI with high Mn content through changes in chemical composition and heat treatment, 5th International Symposium on the Physical Metallurgy of Cast Iron, October 1994, Nancy, France, (1994).

[21] M. Nili Ahamadabadi, E. Niyama, T. Ohide, Structural control of 1% Mn ADI aided by modeling of microsegregation, Transactions AFS, p. 269 (1994).

[22] B. Corlu et al., Microstructure and mechanical properties of austempered Cu-V ductile iron. 2nd International Conference on ADI, University of Michigan, Ann Arbor, 17-19 March, p. 187 (1986).

[23] K. Głownia, A. Gwiżdż, Z. Pirowski Z., J. Wodnicki, Nitrogen and boron effect on structural transformations taking place in ductile iron during austempering treatment, Transactions of the Foundry Research Institute 1, 5 (2010).

[24] G. Gumienny, Carbidic bainitic and ausferritic ductile cast iron, Archives of Metallurgy and Materials **58**, (4), 1053-1058 (2013).

[25] G. Gumienny, T. Giętka, Continuous Cooling Transformation (CCT) Diagrams of Carbidic Nodular Cast Iron, Archives of Metallurgy and Materials **60**, (2) (2015).

[26] F. Zanardi, Machinable ADI In Italy. AFS Transactions, 383 (2005).

Received: 20 January 2015.